

Lattice calculation of $\chi_{c0} \rightarrow 2\gamma$ decay width

Zuoheng Zou,¹ Yu Meng,^{1,2} and Chuan Liu^{1,2,3}

¹*School of Physics, Peking University, Beijing 100871, China*

²*Center for High Energy Physics, Peking University, Beijing 100871, China*

³*Collaborative Innovation Center of Quantum Matter, Beijing 100871, China*

(Dated: January 11, 2022)

We perform a lattice QCD calculation of the $\chi_{c0} \rightarrow 2\gamma$ decay width using a model-independent method which does not require a momentum extrapolation of the corresponding off-shell form factors. The simulation is performed on ensembles of $N_f = 2$ twisted mass lattice QCD gauge configurations with three different lattice spacings. After a continuum extrapolation, the decay width is obtained to be $\Gamma_{\gamma\gamma}(\chi_{c0}) = 3.65(83)_{\text{stat}}(21)_{\text{lat. syst}}(66)_{\text{syst}}$ keV. Albeit this large statistical error, our result is compatible with the experimental results within 1.3σ . Potential improvements of the lattice calculation in the future are also discussed.

PACS numbers: 12.38.Gc, 11.15.Ha

Keywords: charmonium, decay width, lattice QCD.

I. INTRODUCTION

Charmonium physics lives in an energy regime where both perturbative and nonperturbative features of quantum chromodynamics (QCD) intertwine. Notably, Charmonium decay has played an important role in establishing the asymptotic freedom of QCD and served as a clean platform to probe the interplay between perturbative and nonperturbative dynamics. In particular, the two photon annihilation rates of charmonium are extremely helpful for the understanding of quark-antiquark interaction and the decay mechanisms [1, 2].

In this paper, we study the two-photon decay width of χ_{c0} , which has been extensively studied from both experimental and theoretical sides. On the experimental side, using the decay of $\psi(3686) \rightarrow \gamma\chi_{c0}, \chi_{c0} \rightarrow \gamma\gamma$, both CLEO-c and BESIII collaborations reported results of the two-photon decay width $\Gamma_{\gamma\gamma}(\chi_{c0})$ [3, 4]:

$$\begin{aligned}\Gamma_{\gamma\gamma}^{\text{CLEO-c}}(\chi_{c0}) &= 2.36(35)_{\text{stat}}(22)_{\text{syst}} \text{ keV} \\ \Gamma_{\gamma\gamma}^{\text{BESIII}}(\chi_{c0}) &= 2.03(8)_{\text{stat}}(14)_{\text{syst}} \text{ keV} \\ \Gamma_{\gamma\gamma}^{\text{PDG}}(\chi_{c0}) &= 2.20(22) \text{ keV}\end{aligned}\quad (1)$$

where the first line from CLEO-c, the second from BESIII and the last line being the PDG quoted value with combined errors. It is expected that more accurate results for these decay width will become available in the near future.

On the theoretical side, it is fair to say that the situation is far from satisfactory. Theoretical results for the decay rate have been obtained using a non-relativistic approximation [5, 6], potential model [7], relativistic quark model [8–11], non-relativistic QCD (NRQCD) factorization [12–18], effective Lagrangian [19], Dyson-Schwinger equations (DSEs) [20], as well as quenched [21] and unquenched lattice calculations [22]. These results are listed in Table I, which scatter quite a lot although all fall in the right ballpark. Note that within the framework of

NRQCD, the leading-order (LO) prediction is close to the experimental measurements, but this process is extremely sensitive to high-order QCD radiative corrections and relativistic corrections. Therefore, only the LO predictions are listed in Table I.

Theoretical computations for $\Gamma_{\gamma\gamma}(\chi_{c0})$ (keV)			
Huang [1]	3.72 ± 1.10	Barbieri [12]	3.5
Barnes [6]	1.56	Schuler [17]	2.50
Gupta [7]	6.38	Lanseberg [19]	5.00
Ebert [8]	2.90	Chen [20]	2.06-2.39
Godfrey [9]	1.29	Crater [23]	3.34-3.96
Bodwin [10]	6.70 ± 2.80	Wang [24]	3.78
Münz [11]	1.39 ± 0.16	Laverty [25]	1.99-2.10
Dudek [21]	$2.41(58)_{\text{stat}}(86)_{\text{syst}}$	CLQCD [22]	$0.93(19)_{\text{stat}}$

Table I. Some theoretical predictions for $\Gamma_{\gamma\gamma}(\chi_{c0})$.

In the last line of Table I, we list two existing lattice QCD results so far. The first one from Dudek *et al* is a quenched lattice computation on a single lattice spacing [21]. The systematic error they quote mainly come from quenching. The second one from CLQCD is an unquenched study using $N_f = 2$ twisted mass fermions at two distinct lattice spacings. The authors found that the lattice artifacts are substantial and only quoted results from a finite lattice spacing, without an error estimate of the finite lattice spacing errors. The number quoted in Table I is the result from the finer lattice spacing [22]. Therefore, in both lattice studies, systematic effects such as finite lattice errors are not fully investigated which was found to be large in the second study [22]. Obviously, in order to fully compare with the upcoming experiments, one needs to work in a theoretical framework that allows an improvable error control and in this respect, lattice computation obviously has an advantage over other phenomenological methods listed in Table I.

In this paper, we try to improve on the existing lattice computation of $\Gamma_{\gamma\gamma}(\chi_{c0})$ in two major aspects: First, in

previous lattice studies, many systematic effects are not yet fully taken into account, the most important of which being the finite lattice spacing effect, which has been observed in Ref. [22]. Second, one normally computed the off-shell form factors at various discrete photon virtualities. In order to obtain the physical decay width, an extrapolation of these results are required, introducing a model-dependent systematic error.

In this work, we have made the following improvements: First, to attack the lattice artifacts, we perform our calculation on ensembles with three different lattice spacings, allowing us to perform a reliable continuum extrapolation. Second, we adopt a novel method to extract the on-shell form factor directly, by-passing the conventional momentum extrapolation and therefore avoids the corresponding model-dependent extrapolation errors. We have also taken the excited-state contamination into consideration, further improving our results on the physical form factor. Similar procedures has been successfully utilized to two-photon decay of η_c [26]. We hope that these improvements could also shed some light on the two-photon decay of χ_{c0} .

This paper is organized as follows. In Sect. II, the methodology for extracting on-shell form factor is introduced. The Sect. III is divided into several parts: In Sect. III A, the information of the configurations and operators used in this work are introduced. In Sect. III B, the mass spectrum of χ_{c0} is presented. In Sect. III C, we give the renormalization factor and the spectrum weight factor. In Sect. III D, numerical results of the form factor in three different lattice spacings are presented. Then in Sect. III E, extrapolation of the results to continuum is performed, yielding our final result for the decay rate. We also compare our result with both experimental and theoretical results. The main sources of error in our work are discussed and possible solutions in the future are proposed.

II. METHODOLOGY

In this section, we outline the methodology for the calculation of two-photon decay width of χ_{c0} . In the traditional approach [27], using the Lehmann-Symanzik-Zimmermann (LSZ) reduction formula and integrating out the QED part to $\mathcal{O}(\alpha_{em})$, the amplitude for two-photon decay of charmonium can be obtained as follows [21],

$$\langle \gamma\gamma | M(p_f) \rangle \sim e^2 \epsilon_\mu^* \epsilon_\nu^* \int dt_i e^{-\omega_1(t_i-t)} \int d^3\vec{x} e^{-i\vec{p}_f \cdot \vec{x}} \int d^3\vec{y} e^{i\vec{q}_2 \cdot \vec{y}} \langle 0 | T \left\{ \varphi_M(\vec{x}, t_f) J_\nu(\vec{y}, t) J_\mu(\vec{0}, t_i) \right\} | 0 \rangle \quad (2)$$

where $\varphi_M(\vec{x}, t_f)$ is an appropriate composite operator which creates a desired meson M (in our case, the χ_{c0} meson) from the QCD vacuum; $\epsilon_\mu, \epsilon_\nu$ are the polarization four-vectors for the two final photons; $J_\mu = \sum_q e_q \bar{q} \gamma_\mu q$

($e_q = 2/3, -1/3, -1/3, 2/3$ for $q = u, d, s, c$) is the electromagnetic current operator due to the quarks, with e being the elementary charge unit. In this work, we only consider the connected contributions arising from the charm quark current. Disconnected contributions are neglected. These contributions are extremely costly for lattice computations and are assumed to be small in charmonium physics [21, 28, 29]. Then, the matrix element in Eq. (2) relevant for χ_{c0} decay can be parameterized in terms of the form factor $G(Q_1^2, Q_2^2)$ as,

$$\langle \gamma(q_1) \gamma(q_2) | M(p_f) \rangle = \frac{2}{m_\chi} \left(\frac{2}{3}e\right)^2 G(Q_1^2, Q_2^2) [\epsilon_1 \cdot \epsilon_2 q_1 \cdot q_2 - \epsilon_2 \cdot q_1 \epsilon_1 \cdot q_2] \quad (3)$$

where q_1, q_2 are the two four-momenta of the final photons while $Q_1^2 = -q_1^2, Q_2^2 = -q_2^2$ are the virtualities of the two photons. The mass of χ_{c0} is denoted as m_χ and the polarization vectors of the two photons are given by ϵ_1 and ϵ_2 . The physical decay width is related to the on-shell form factor which is obtained by a momentum extrapolation towards the physical point: $Q_1^2 = Q_2^2 = 0$. Thus, in this conventional approach, in order to have a better control on the extrapolation, one needs to compute the matrix element at various different non-physical virtuality combinations, thereby also introducing extra computational costs. The extrapolation itself also brings about model-dependent systematic errors. In the new approach introduced in this work, we adopt a method that requires no off-shell form factor calculations at all and therefore by-passing the model-dependent extrapolation in photon virtualities. The method has been successfully utilized in two-photon decays of η_c [26]. We now briefly outline the major steps for the case of χ_{c0} below.

One first relates the on-shell decay amplitude of $\chi_c \rightarrow 2\gamma$ to an infinite-volume hadronic tensor $\mathcal{F}_{\mu\nu}(p)$ which is the Fourier transform of the real-space tensor $\mathcal{H}_{\mu\nu}(t, \vec{x})$ in continuum Euclidean space,

$$\mathcal{F}_{\mu\nu}(p) = \int dt e^{m_\chi t/2} \int d^3\vec{x} e^{-i\vec{p} \cdot \vec{x}} \mathcal{H}_{\mu\nu}(t, \vec{x}), \quad (4)$$

$$\mathcal{H}_{\mu\nu}(t, \vec{x}) = \langle 0 | T J_\mu(x) J_\nu(0) | \chi_{c0}(k) \rangle,$$

where we have chosen the rest-frame of the χ_{c0} meson so that $k = (im_\chi, \vec{0})$. Note that we have fixed the four-momentum for one of the final photons to be $p = (im_\chi/2, \vec{p})$ with $|\vec{p}| = m_\chi/2$, making it on-shell explicitly and energy-momentum conservation then guarantees the other photon with four-momentum p' is also on-shell. With this choice, the on-shell decay amplitude may be written as,

$$M = e^2 \epsilon_\mu^*(p, \lambda) \epsilon_\nu^*(p', \lambda') \mathcal{F}_{\mu\nu}(p) \quad (5)$$

According to the quantum number of χ_{c0} , the hadronic tensor can be parameterized as (repeated indices are summed),

$$\mathcal{F}_{\mu\nu}(p) = \epsilon_{ij\mu\alpha} \epsilon_{ij\nu\beta} p_\alpha k_\beta F_{\chi_{c0}\gamma\gamma}. \quad (6)$$

The approach to extract the on-shell form factor $F_{\chi_{c0}\gamma\gamma}$ here is also slightly different from the conventional one.

By further multiplying the Lorentz structure factor in the above equation, the hadronic tensor can be contracted to a scalar including only the form factor $F_{\chi_{c0}\gamma\gamma}$ with a constant factor. Then the form factor can be derived by dividing the coefficient as follows,

$$\begin{aligned} F_{\chi_{c0}\gamma\gamma} &= \frac{\epsilon_{ij\mu\alpha}\epsilon_{ij\nu\beta}p_\alpha k_\beta \mathcal{F}_{\mu\nu}(p)}{\epsilon_{ij\mu\alpha}\epsilon_{ij\nu\beta}p_\alpha k_\beta \epsilon_{i'j'\mu\alpha'}\epsilon_{i'j'\nu\beta'}p_{\alpha'}k_{\beta'}} \\ &= -\frac{1}{8m_\chi|\vec{p}|^2} \int dt e^{m_\chi t/2} \\ &\quad \times \int d^3\vec{x} e^{-i\vec{p}\cdot\vec{x}} \epsilon_{ij\mu\alpha}\epsilon_{ij\nu\beta} \frac{\partial \mathcal{H}_{\mu\nu}(x)}{\partial x_\alpha} \end{aligned} \quad (7)$$

Until now, all derivations are in the continuum Euclidean space. We now utilize the spatial isotropy symmetry to average over the spatial direction of \vec{p} ,

$$\begin{aligned} e^{-i\vec{p}\cdot\vec{x}} &\rightarrow \frac{1}{4\pi} \int d\Omega_{\vec{p}} e^{-i\vec{p}\cdot\vec{x}} = \frac{\sin(|\vec{p}||\vec{x}|)}{|\vec{p}||\vec{x}|} \equiv j_0(|\vec{p}||\vec{x}|) \\ \frac{d}{dz}(j_0(z)) &= -\left(\frac{\sin z}{z^2} - \frac{\cos z}{z}\right) \equiv -j_1(z), \end{aligned} \quad (8)$$

where $j_n(x)$ are the spherical Bessel functions. Finally the scalar form factor is expressed as

$$\begin{aligned} F_{\chi_{c0}\gamma\gamma} &= \frac{1}{8m_\chi} \int dt e^{m_\chi t/2} \int d^3\vec{x} \\ &\quad \times \left[\frac{j_1(|\vec{p}||\vec{x}|)}{|\vec{p}||\vec{x}|} (x_i \mathcal{H}_{0i} + x_i \mathcal{H}_{i0}) + \frac{j_0(|\vec{p}||\vec{x}|)}{|\vec{p}|} 2\mathcal{H}_{ii} \right] \end{aligned} \quad (9)$$

where $i = 1, 2, 3$ take spatial indices and are assumed to be summed over.

To obtain the hadronic tensor $\mathcal{H}_{\mu\nu}(t, \vec{x})$ in Eq. (9), we utilize the variational method to find the optimal interpolation operators to create the χ_{c0} meson state [30]. The physical decay width of χ_{c0} is given by

$$\Gamma_{\gamma\gamma}(\chi_{c0}) = \alpha^2 \pi m_{\chi_{c0}}^3 F_{\chi_{c0}\gamma\gamma}^2. \quad (10)$$

Therefore, one only needs to compute the Euclidean correlation functions \mathcal{H}_{0i} and \mathcal{H}_{ii} that are directly relevant for the on-shell amplitude and substitute the results into Eq. (9) to arrive at the physical decay width $\Gamma_{\gamma\gamma}(\chi_{c0})$ in Eq. (10). This completely avoids the on-shell extrapolation process in the conventional lattice approach.

III. SIMULATION RESULTS

A. Lattice setup

We utilize three $N_f = 2$ -flavor twisted mass gauge field ensembles generated by the Extended Twisted Mass Collaboration (ETMC) with lattice spacing $a \simeq 0.0667, 0.085, 0.098$ fm, respectively. The parameters of these ensembles are presented in Table. II. The valence charm quark mass parameter m_c is tuned so that the mass of the η_c meson for each ensemble reproduces its correct

Ensemble	a (fm)	$L^3 \times T$	N_{conf}	$a\mu_l$	m_π (MeV)	t_h
Ens.I	0.067(2)	$32^3 \times 64$	179	0.003	300	10-20
Ens.II	0.085(3)	$24^3 \times 48$	200	0.004	315	10-15
Ens.III	0.098(3)	$24^3 \times 48$	216	0.006	365	10-15

Table II. From left to right, we list the ensemble name, the lattice spacing a , the spatial and temporal lattice size L and T , the number of the measurements of the correlation function for each ensemble $N_{\text{conf}} \times T$, the light quark mass $a\mu_l$, the pion mass m_π and the range of the time separation t_h between χ_{c0} and photon.

physical value. For more details, we refer the reader to Ref. [31, 32],

Before getting into the simulation details, there remains one subtlety to clarify that is related to the twisted mass fermion. Since the twisted mass action breaks parity \mathcal{P} by $\mathcal{O}(a^2)$ effects, the basis operator $\mathcal{O}_1 = \bar{c}c$ for χ_{c0} would unfortunately mix with $\mathcal{O}_2 = \bar{c}\gamma^5 c$ which has the opposite parity. This mixing implies that a specific combination of these operators will be relevant to create a physical scalar charmonium in the twisted mass action [30]

$$\mathcal{O}_{\chi_{c0}}^\dagger = v_1^\chi \mathcal{O}_1^\dagger + v_2^\chi \mathcal{O}_2^\dagger \quad (11)$$

The two-point correlation function $C_{\chi_{c0}}(t) = \langle 0 | \mathcal{O}_{\chi_{c0}}(t) \mathcal{O}_{\chi_{c0}}^\dagger(0) | 0 \rangle$ can be derived by multiplying the corresponding coefficients with the basis correlation functions $C'_{ij} = \langle 0 | \mathcal{O}_i(t) \mathcal{O}_j^\dagger(0) | 0 \rangle$ ($i, j = 1, 2$). Therefore, after choosing a time slice t_0 , one could disentangle the mixing of the two operators by solving a generalized eigenvalue problem (so-called GEVP procedure):

$$\begin{aligned} &\begin{pmatrix} C'_{11}(t) & C'_{12}(t) \\ C'_{21}(t) & C'_{22}(t) \end{pmatrix} \begin{pmatrix} v_1^\chi & v_1^\eta \\ v_2^\chi & v_2^\eta \end{pmatrix} \\ &= \begin{pmatrix} \lambda_1 & 0 \\ 0 & \lambda_2 \end{pmatrix} \begin{pmatrix} C'_{11}(t_0) & C'_{12}(t_0) \\ C'_{21}(t_0) & C'_{22}(t_0) \end{pmatrix} \begin{pmatrix} v_1^\chi & v_1^\eta \\ v_2^\chi & v_2^\eta \end{pmatrix} \end{aligned} \quad (12)$$

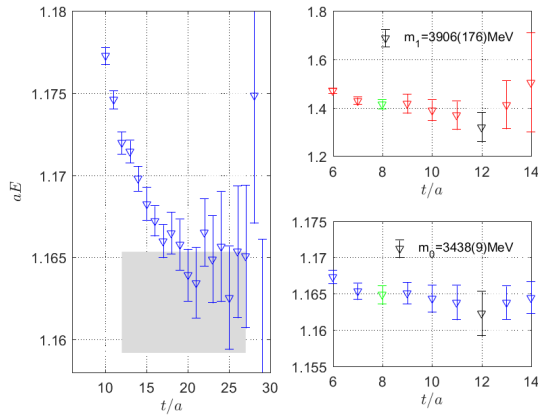
where the generalized eigenvalues λ_i behave like $e^{-E_i(t-t_0)}$ at large time separation. In practice, we fix $t_0 = 1$ and solve Eq. (12) on each time-slice independently and use them to reconstruct the three-point correlation functions.

B. Mass spectrum for χ_{c0}

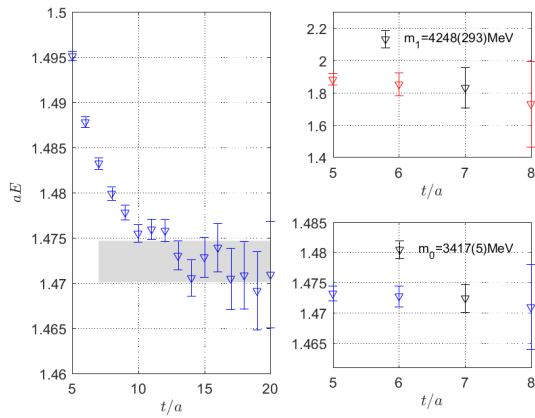
Since the generalized eigenvalues in Eq. (12) decay exponentially, the corresponding mass eigenvalues can be extracted easily from,

$$\cosh(m_n) = \frac{\lambda_n(t-1) + \lambda_n(t+1)}{2\lambda_n(t)}. \quad (13)$$

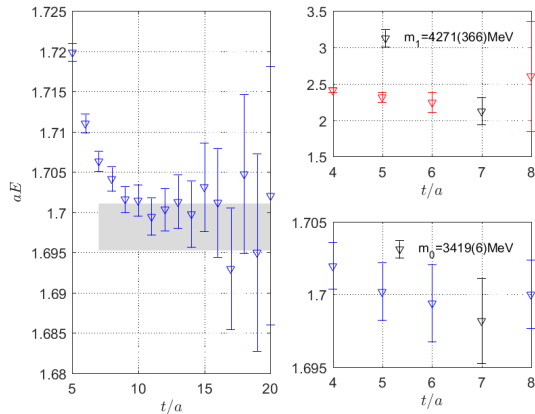
Since we want to extrapolate the form factor to eliminate the excited state contamination, we therefore use



(a) Ens.I



(b) Ens.II



(c) Ens.III

Figure 1. The left panels show the effective mass at different time slices together with the corresponding fitting ranges (grey bands) and the right panels are the ground and excited state mass values fitted from two-point correlation functions using Eq. (14). The black symbols denote the chosen m_0 , that correspond to the grey band to its left. The green symbols in (a) denote another choice for the m_0 and m_1 .

the following two-state fit form for the χ_{c0} correlator,

$$C_{\chi_{c0}}^{(2)}(t) = V \sum_{i=0,1} \frac{Z_i^2}{2m_i} \left(e^{-m_i t} + e^{-m_i(T-t)} \right) \quad (14)$$

with V being the spatial volume, m_0 the ground state mass and m_1 the first excited state mass. The factors $Z_i = \frac{1}{\sqrt{V}} \langle i | \mathcal{O}_{\chi_{c0}}^\dagger | 0 \rangle$ (with $i = 0, 1$) are the overlap amplitudes for the ground and the first excited state, respectively. The corresponding mass plateaus and the masses are illustrated in Fig. 1 for the three ensembles we utilize in this work. The left column of the panels show the effective mass on each time slice. The right panels denote the mass values fitted from two-point correlation functions, the upper one for the first excited state and the bottom one for the ground state. As the grey bands in the left panels indicate, the starting time slices are adjusted according to $\chi^2/d.o.f$ of the fit while the ending time slices are fixed to be $t_{\max} = 27, 20, 20$ for ensemble I, II, III, respectively. Noting that the grey band of Ens.I is obviously different from the other two ensembles, the ground state mass m_0 might be underestimated. So we calculate the result for another plateau with green mark and take the difference of them as the major source of systematic uncertainty.

The results for the mass values are summarized in Table III. Note that we use the η_c mass to fix the valence charm quark mass $a\mu_c$ in this work. And the χ_{c0} experiment mass is 3414.7(3)MeV quoted by PDG [33].

Table III. Mass value m_0 and spectral weight Z_0 for ground state and the first excited state mass m_1 on each ensemble respectively. Ens.I(a) and Ens.I(b) are corresponding to the black and green symbols respectively.

	m_0 [MeV]	Z_0	m_1 [MeV]
Ens.I(a)	3438(9)	0.0959(25)	3906(176)
Ens.I(b)	3445(4)	0.0972(9)	4181(57)
Ens.II	3417(5)	0.1216(10)	4248(293)
Ens.III	3419(6)	0.1320(7)	4271(366)

C. Renormalization factor Z_V

The hadronic tensor $\mathcal{H}_{\mu\nu}$ contains the electromagnetic current operators J_μ from all flavor of quarks. However, since we neglect the disconnected diagrams in this study, we only need to consider the charm quark current $J_\mu^{(c)} = \bar{c}\gamma_\mu c(\vec{x}, t)$. Since we adopt the local current form, there exists an extra multiplicative renormalization factor Z_V that can be calculated by a ratio of the two-point function and the three-point function as in Eq. (15). In principle this renormalization factor does not depend on the particle state used to calculate it. For a better signal, we choose to use the η_c correlators instead of χ_{c0} .

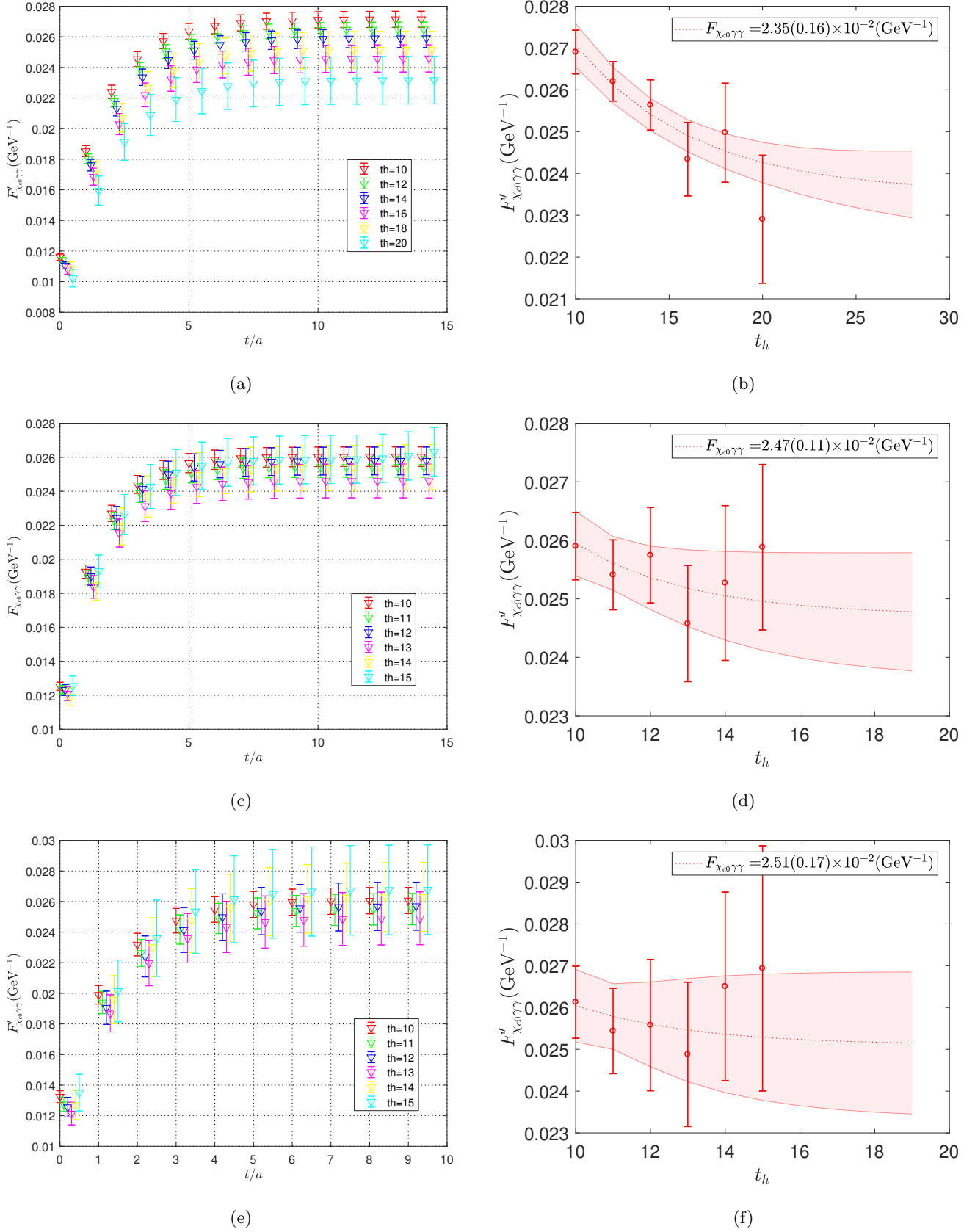


Figure 2. The left column represents the plateaus of the form factor with different t_h while the right column shows the extrapolation to the ground state contribution. The label (a) and (b), (c) and (d), (e) and (f) are for Ens.I(a), Ens.II, Ens.III respectively.

Taking account of the around-of-world effect, we use the following relation to extract Z_V .

$$Z_V = \frac{\sum_{\vec{x}} \langle \mathcal{O}_{\eta_c}(t) \mathcal{O}_{\eta_c}^\dagger(0) \rangle}{\sum_{\vec{x}} \langle \mathcal{O}_{\eta_c}(t) J_0^{(c)}(t/2, \vec{x}) \mathcal{O}_{\eta_c}^\dagger(0) \rangle} \frac{1}{(1 + e^{-m_0(T-2t)})} \quad (15)$$

The results for Z_V are listed in Table IV.

	Ens.I	Ens.II	Ens.III
Z_V	0.6523(21)	0.6296(29)	0.6057(27)

Table IV. Renormalization factor Z_V for three ensembles.

When computing the scalar form factor $F_{\chi_{c0}\gamma\gamma}$ in Eq. (9) on the lattice, the integration over space-time are replaced by discrete summations. When two identical currents in $\mathcal{H}_{\mu\nu}(t, \vec{x})$, meaning that they share the same Lorentz index, are at the same space-time point, an extra renormalization is needed to take into account of the contact term. This is due to a new type of composite operator that is not properly renormalized yet, even if each current is already properly renormalized by the factor Z_V . In order to take this effect into account, one needs to impose another appropriate renormalization condition for this new composite operator. In this work, we choose not to sum the same space-time point contributions for identical currents and thereby avoiding this potential renormalization. To summarize, the above mentioned procedures taken on already $O(a)$ -improved ensembles will at most introduce an extra $O(a^2)$ lattice artifact on physical observables which will be taken care of in the final continuum extrapolation.

D. The scalar form factor $F_{\chi_{c0}\gamma\gamma}$

When computing the hadronic tensor, we evaluate the three-point correlation function $\langle J_\mu(x) J_\nu(0) \mathcal{O}_{\chi_{c0}}^\dagger(-t_h) \rangle$. To produce the static meson state, we use the Z_4 -stochastic wall source placed at time-slice $-t_h$. This cuts the uncertainty by nearly a half when compared with the simple point source for the meson mass. We also apply the APE [34] and Gaussian smearing [35] for the gauge field and χ_{c0} operator. We utilize the random point source propagator for the current to arrive at the three-point correlation function. In practice, the hadronic tensor with current $J_\nu(0)$ placed at zero point is actually an average of all the time slices and a random positions on each time slice.

Consequently, the scalar form factor we computed according to Eq. (9) on the lattice $F'_{\chi_{c0}\gamma\gamma}$ actually suffers from excited state contamination due to higher excitation states of χ_{c0} . What we really need is the ground state χ_{c0} . This effect can be taken care of by considering t_h dependence of the form factors. Therefore, we computed several different separations t_h and perform the following

fit,

$$F'_{\chi_{c0}\gamma\gamma}(t_h) = F_{\chi_{c0}\gamma\gamma} + \xi \cdot e^{-(m_1-m_0)t_h}, \quad (16)$$

where $F_{\chi_{c0}\gamma\gamma}$ and ξ are the two free parameters. For the parameters m_0 and m_1 , we take the values presented in Table III. The form factor with different time separation t_h together with the ground state extrapolation values for $F_{\chi_{c0}\gamma\gamma}$ for three set of ensembles are illustrated in Fig. 2.

E. Comparison of the form factor with previous lattice results

The most recent lattice computation on $\chi_{c0} \rightarrow \gamma\gamma$ decay in the literature is the one from CLQCD [22], which happened to use exactly the same set of ensembles as this work. This allows a more detailed comparison on the level of dimensionless form factors for each of the common lattice spacings. For this purpose, we decide to convert our results for $F_{\chi_{c0}\gamma\gamma}$ into dimensionless quantities which could be taken as either $\Gamma_{\gamma\gamma}(\chi_{c0})/m_{\chi_{c0}}$ or the dimensionless form factor $G(0,0)$ that is utilized in Ref. [22]. The relation between these two dimensionless quantities is easily found to be,

$$\frac{\Gamma_{\gamma\gamma}(\chi_{c0})}{m_{\chi_{c0}}} = \alpha^2 \pi |m_{\chi_{c0}} F_{\chi_{c0}\gamma\gamma}|^2 = \alpha^2 \pi (e_c)^4 |G(0,0)|^2. \quad (17)$$

Dimensionless quantities have the advantage that they are independent of the scale setting process for the lattice spacings, which is subject to its own errors depending on how the scale was set. Since the scale setting processes for lattice calculations also progress over the years, the information for the lattice spacing in physical units, both the central values and the errors, are also changing with time even for a given particular ensemble. It is therefore better to attach these errors due to scale-setting at the very end when comparing with the experiments. In the intermediate step when comparing with other lattice computations, it is easier to directly compare the dimensionless quantities if possible. In fact, this allows us to compare with previous lattice results in Ref. [22] at each individual lattice spacing, namely Ens.I and Ens.II that have also been utilized. Of course, when quoting the final physical decay width, the effect of scale setting will be taken into account together with its associated errors.

In Table V, the dimensionless form factor $G(0,0)$ obtained via Eq. (17) from $F_{\chi_{c0}\gamma\gamma}$ for all three ensembles are listed together with the corresponding results for Ens.I and Ens.II from Ref. [22]. Ens.III was not utilized in the study of Ref. [22]. Two entries for Ens.I, labelled as Ens.I(a) and Ens.I(b) corresponds to the two different ways of extracting χ_{c0} masses as discusses in Fig. 1. The errors quoted for $G(0,0)$ in this work are obtained using the conventional jackknife method. As for the three errors for the results from Ref. [22], they stand for errors from statistical, from momentum extrapolations and estimates of the finite lattice spacing errors, respectively.

$G(0,0)$	Ens.I(a)	Ens.I(b)	Ens.II	Ens.III
This work	0.1884(123)	0.1899(69)	0.1911(85)	0.1931(131)
Ref.[22]	0.09079(8)(19)(90)		0.1017(7)(102)(126)	-

Table V. Dimensionless form factors $G(0,0)$ obtained in this work and those obtained in Ref. [22] for each ensemble. Ens.I(a) and Ens.I(b) denotes two different results obtained by taking two different χ_{c0} mass values as discussed in Fig. 1. Ensemble III was not available in Ref.[22]. Errors quoted for $G(0,0)$ in this work are purely statistical that are obtained using the conventional jackknife method. Three errors for the results from Ref.[22] stands for errors from statistical, from momentum extrapolations and estimates for the finite lattice spacings.

We notice that the central values for dimensionless form factors $G(0,0)$ differ by almost a factor of two for Ens.I and Ens.II. The reason of this apparent discrepancy is still unknown to us. One possibility could be the under estimation of the lattice artifacts for each of the ensemble in Ref. [22].

F. Continuum extrapolation and the final result and discussions

After obtaining the dimensionless form factors for three different lattice spacings, we could investigate the continuum limit of this quantity. For this purpose, we decide to perform this extrapolation using the more physical quantity $\Gamma_{\gamma\gamma}(\chi_{c0})/m_{\chi_{c0}}$, which is proportional to the norm-squared dimensionless form factor $|G(0,0)|^2$ as indicated in Eq. (17). The continuum extrapolation is done by performing a linear fit in a^2 for the three ensembles and the result after the continuum extrapolation, together with the results for each ensemble, are illustrated in Fig. 3. Here the horizontal error bars for the data points indicate the errors in a^2 inferred from Ref. [31, 32]

It is seen that the three data points fit nicely on a straight line yielding a reasonable $\chi^2/d.o.f.$. The two points near $a^2 = 0$ with larger error bars designate two different results obtained from the fit with and without considering the horizontal a^2 -errors for the lattice spacings. Below the two data points, we also plot the corresponding experimental value from PDG for this ratio. The two extrapolated results share almost identical central values. They differ only by their errors. The point with slightly larger error (the one slightly to the left) is the one that takes into account of the horizontal a^2 -errors while the other one is the one without considering a^2 -errors. Finally, there is another source of systematic errors arising from the different plateaus in the mass as discussed in Sec. IIIB. Therefore, we finally quote the result of the decay width in physical units as

$$\Gamma_{\gamma\gamma}(\chi_{c0}) = 3.65(83)_{\text{stat}}(21)_{\text{lat.syst}}(66)_{\text{syst}} \text{ keV}, \quad (18)$$

where the first two errors represent the error obtained without/with the a^2 -errors. It should be interpreted as follows: the first error is the error without considering a^2 -errors. The second one with the subscript *lat.syst* indicate the extra amount of error if one would consider the a^2 -errors. In other words, one could add the first

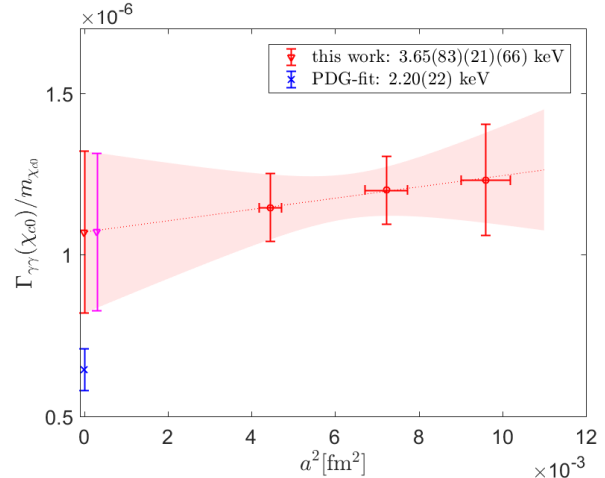


Figure 3. Continuum extrapolation for the ratio $\Gamma_{\gamma\gamma}(\chi_{c0})/m_{\chi_{c0}}$. The three data points with both horizontal and vertical error-bars are results from three ensembles. The extrapolated results are shown by two side-by-side points near $a^2 = 0$: The one with a smaller error bar (the right one) represents the extrapolation result without considering lattice spacing errors. The other one (left one) is the result with lattice spacing errors taken into consideration. The data point (blue) below these two with a smaller error is the PDG-fit value for this ratio. At the upper right corner, we have also indicated the result of the width in physical units.

two errors in quadrature to obtain the error with a^2 -errors taken into consideration, which is shown by the left point near $a^2 = 0$ in Fig. 3. The last error with subscript *syst* reflects the systematic error from different mass plateaus in Ens.I(a) and Ens.I(b). In this manner, we separate different sources of systematic errors that have been studied in this paper.

It is evident that the central value for the decay width obtained in this paper is larger than the PDG value. But due to our large statistical and systematical uncertainty, it is still compatible with the experimental results within 1.3σ .

We have tried to estimate the systematic uncertainties that might influence our final result quoted above in Eq. (18). This includes choosing different plateaus for the mass, for the renormalization factor Z_V , spectral weight factor Z_i , and the number of time-slices we choose for the extrapolation of the ground state form fac-

tor, etc. It turns out that only the two plateaus presented in Sec. III B contribute to a visible deviation in the central value, which we add in the third error in Eq. 18.

Needless to say, there are also other source of systematic errors that are more difficult to quantify, say neglecting the disconnected contributions, quenching of the the strange and charm quarks, etc. The disconnected diagrams contributions are believed to be suppressed in the charmonium system [28, 29] due to the Okubo-Zweig-Iizuka(OZI) rule. Furthermore, the non-physical masses of up and down quarks usually only result in a small effect which is indicated in the previous lattice calculations [36]. Therefore, the major direction in future improvements points to the deduction of the statistical noise in χ_{c0} correlation functions. Only after the large statistical uncertainty is fully under control, should we worry about other remaining systematic effects.

Part of the large statistical error in our study can be traced back to the mixing of χ_{c0} and η_c in the twisted-mass formulation of lattice QCD. To entangle this mixing, we have utilized a GEVP procedure that projects out the operators best overlapped with η_c and χ_{c0} as discussed in Sec. III A. Although this procedure works perfectly for the ground state η_c , the efficiency for χ_{c0} is not quite satisfactory, rendering the two-point and three-point correlation functions of χ_{c0} much noisier than that of η_c , resulting in a much larger error for the decay rate of χ_{c0} . Possibilities to get around this difficulty could be simply increasing the statistics of the ensembles, using more interpolating operators as the basis operators or simply using a formulation that does not suffer from this mixing effect at all, e.g. utilizing the clover-improved Wilson fermion configurations.

IV. CONCLUSION

In this paper, we report a new lattice QCD computation of the scalar charmonium χ_{c0} to two-photon decay width. We have performed our study using three ensembles of $N_f = 2$ twisted mass gauge field configurations at three different lattice spacings. This allows us to perform a more reliable continuum extrapolation therefore eliminating the substantial finite lattice spacing errors observed in previous lattice studies. We also adopt a new method that directly extracts the relevant on-shell form factor, by-passing the extrapolation in the photon virtualities. We obtain the decay width of χ_{c0} meson to be $\Gamma_{\gamma\gamma}(\chi_{c0}) = 3.65(83)_{\text{stat}}(21)_{\text{lat.syst}}(66)_{\text{syst}}$ keV. Albeit the large errors in this computation, the result is compatible with the existing experimental values within 1.3σ . Further possible improvements are also discussed. This calculation and possible future more systematic studies will await the new experimental results that will become available soon.

ACKNOWLEDGMENTS

The authors would like to thank the Extended Twisted Mass Collaboration(ETMC) for sharing the gauge configurations with us. C.L. and Z.H.Z. acknowledge the support by NSFC of China under Grant No. 12070131001 and also the support by CAS Interdisciplinary Innovation Team and NSFC of China under Grant No. 11935017. Y.M. are supported by NSFC of China under Grant No. 12047505 and State Key Laboratory of Nuclear Physics and Technology, Peking University. The calculations were carried out on High-performance Computing Platform of Peking University and Tianhe-1A supercomputer at Tianjin National Supercomputing Center.

-
- [1] H.-W. Huang, C.-F. Qiao, and K.-T. Chao, Electromagnetic annihilation rates of χ_{c0} and χ_{c2} with both relativistic and qcd radiative corrections, Phys. Rev. D **54**, 2123 (1996).
 - [2] C.-W. Hwang and R.-S. Guo, Two-photon and two-gluon decays of p -wave heavy quarkonium using a covariant light-front approach, Phys. Rev. D **82**, 034021 (2010).
 - [3] K. M. Ecklund *et al.* (CLEO Collaboration), Two-photon widths of the χ_{cJ} states of charmonium, Phys. Rev. D **78**, 091501 (2008).
 - [4] M. Ablikim *et al.* (BESIII Collaboration), Improved measurements of two-photon widths of the χ_{cJ} states and helicity analysis for $\chi_{c2} \rightarrow \gamma\gamma$, Phys. Rev. D **96**, 092007 (2017).
 - [5] T. Appelquist and H. D. Politzer, Heavy quarks and e^+e^- annihilation, Phys. Rev. Lett. **34**, 43 (1975).
 - [6] T. Barnes, *Proceedings of the IX International Workshop on Photon-Photon Collisions*, edited by D. O. Caldwell and H. P. Paar(World Scientific, Singapore, 1992) p. 263.
 - [7] S. N. Gupta, J. M. Johnson, and W. W. Repko, Relativistic two-photon and two-gluon decay rates of heavy quarkonia, Phys. Rev. D **54**, 2075 (1996).
 - [8] D. Ebert, R. Faustov, and V. Galkin, Two-photon decay rates of heavy quarkonia in the relativistic quark model, Mod.Phys.Lett.A **18**, 601 (2003).
 - [9] S. Godfrey and N. Isgur, Mesons in a relativized quark model with chromodynamics, Phys. Rev. D **32**, 189 (1985).
 - [10] G. T. Bodwin, E. Braaten, and G. P. Lepage, Rigorous qcd predictions for decays of p -wave quarkonia, Phys. Rev. D **46**, R1914 (1992).
 - [11] C. R. Munz, Two photon decays of mesons in a relativistic quark model, Nucl. Phys. A **609**, 364 (1996), arXiv:hep-ph/9601206.
 - [12] R. Barbieri, R. Gatto, and R. Kögerler, Calculation of the annihilation rate of p wave quark-antiquark bound states, Physics Letters B **60**, 183 (1976).
 - [13] R. Barbieri, M. Caffo, R. Gatto, and E. Remiddi, Strong qcd corrections to p-wave quarkonium decays, Physics Letters B **95**, 93 (1980).
 - [14] R. Barbieri, M. Caffo, R. Gatto, and E. Remiddi, Qcd corrections to p wave quarkonium decays, Nuclear Physics B **192**, 61 (1981).

- [15] J. Ma and Q. Wang, Corrections for two photon decays of χ_{c0} and χ_{c2} and color octet contributions, *Physics Letters B* **537**, 233 (2002).
- [16] N. Brambilla, E. Mereghetti, and A. Vairo, Electromagnetic quarkonium decays at order v^7 , *Journal of High Energy Physics* **2006**, 039 (2006).
- [17] G. Schuler, F. Berends, and R. van Gulik, Meson-photon transition form factors and resonance cross-sections in e^+e^- collisions, *Nuclear Physics B* **523**, 423 (1998).
- [18] W.-L. Sang, F. Feng, Y. Jia, and S.-R. Liang, Next-to-next-to-leading-order qcd corrections to $\chi_{c0,2} \rightarrow \gamma\gamma$, *Phys. Rev. D* **94**, 111501 (2016).
- [19] J. P. Lansberg and T. N. Pham, Effective lagrangian for two-photon and two-gluon decays of p -wave heavy quarkonium $\chi_{c0,2}$ and $\chi_{b0,2}$ states, *Phys. Rev. D* **79**, 094016 (2009).
- [20] J. Chen, M. Ding, L. Chang, and Y.-x. Liu, Two-photon transition form factor of $\bar{c}c$ quarkonia, *Phys. Rev. D* **95**, 016010 (2017).
- [21] J. J. Dudek and R. G. Edwards, Two-photon decays of charmonia from lattice qcd, *Phys. Rev. Lett.* **97**, 172001 (2006).
- [22] Y. Chen *et al.* (CLQCD Collaboration), Lattice study of two-photon decay widths for scalar and pseudo-scalar charmonium, *Chinese Physics C* **44**, 083108 (2020).
- [23] H. W. Crater, C.-Y. Wong, and P. Van Alstine, Tests of two-body dirac equation wave functions in the decays of quarkonium and positronium into two photons, *Phys. Rev. D* **74**, 054028 (2006).
- [24] G.-L. Wang, Annihilation rate of heavy 0^{++} p-wave quarkonium in relativistic salpeter method, *Physics Letters B* **653**, 206 (2007).
- [25] J. T. Lavery, S. F. Radford, and W. W. Repko, $\gamma\gamma$ and g g decay rates for equal mass heavy quarkonia (2011), arXiv:0901.3917 [hep-ph].
- [26] Y. Meng, X. Feng, C. Liu, T. Wang, and Z. Zou, First-principle calculation of $\eta_c \rightarrow 2\gamma$ decay width from lattice qcd, (2021), arXiv:2109.09381 [hep-lat].
- [27] X. Ji and C. Jung, Studying hadronic structure of the photon in lattice qcd, *Phys. Rev. Lett.* **86**, 208 (2001).
- [28] C. McNeile and C. Michael (UKQCD Collaboration), Estimate of the flavor singlet contributions to the hyperfine splitting in charmonium, *Phys. Rev. D* **70**, 034506 (2004).
- [29] P. Forcrand *et al.* (The QCD-TARO Collaboration), Contribution of disconnected diagrams to the hyperfine splitting of charmonium, *JHEP* **2004** (08), 004.
- [30] C. J. Shultz, J. J. Dudek, and R. G. Edwards (for the Hadron Spectrum Collaboration), Excited meson radiative transitions from lattice qcd using variationally optimized operators, *Phys. Rev. D* **91**, 114501 (2015).
- [31] P. Boucaud *et al.*, Dynamical twisted mass fermions with light quarks: simulation and analysis details, *Comput. Phys. Commun.* **179**, 695 (2008).
- [32] B. Blossier, P. Dimopoulos, R. Frezzotti, V. Lubicz, M. Petschlies, F. Sanfilippo, S. Simula, and C. Tarantino, Average up/down, strange, and charm quark masses with $N_f = 2$ twisted-mass lattice qcd, *Phys. Rev. D* **82**, 114513 (2010).
- [33] P. Zyla *et al.* (Particle Data Group), Review of Particle Physics, *PTEP* **2020**, 083C01 (2020).
- [34] M. Albanese *et al.* (APE Collaboration), Glueball masses and string tension in lattice qcd, *Phys. Lett. B* **192**, 163 (1987).
- [35] S. Gusken, A Study of smearing techniques for hadron correlation functions, *Nucl. Phys. B Proc. Suppl.* **17**, 361 (1990).
- [36] G. Bali, S. Collins, *et al.*, Spectra of heavy-light and heavy-heavy mesons containing charm quarks, including higher spin states for $n_f = 2 + 1$, *PoS LATTICE2011*, 135 (2011), arXiv:1108.6147 [hep-lat].